2019 IEEE 15th International Conference on Control and Automation (ICCA)
Edinburgh, Scotland, July 16-19, 2019

Bearing-based Bionic Encirclement Control Inspired by Dolphins

Zhiwen Zeng, Xiangke Wang*, Huimin Lu, Junhao Xiao, Zhiqiang Zheng
Department of Automation
College of Intelligence Science and Technology
National University of Defense Technology

***Abstract*—Inspired by the encirclement behavior of dolphins to entrap fishes, we investigate the bionic encirclement control by employing the bearing rigidity theory. To begin with, we transform the encirclement problem into target formation with time-varying bearing constraint. Then, to achieve a dynamic circle to entrap the target as well as gradually tighten the encirclement, we propose a distributed control law by combining orthogonal projection operator and the consensus protocol. In addition, we analyze the stability of the coordination tasks by using Lyapunov method and small-gain theorem. Moreover, we figure out that the shrinkage of the formation scale is according to exponential law and also provide the estimates of the tightening rate. Finally, simulation results are given to verify the theoretical analysis.**

***Index Terms*—encirclement control, bearing rigidity, consensus, small-gain**

I. Introduction

Researchers have long noticed many interesting coordinated behaviors in nature, for example, the forage for food or defense against predators of insects, birds and fishes. These behaviors attracted researchers to consider seriously why the creature take initiative to coordinate, and motivated the theoretical and applied studies on multi-agent coordination.

Inspired by the death-vortex phenomenon of ants as shown in [1], a simple coordination strategy which is called as cyclic pursuit aroused great interesting from the researchers. In [2], Marshall et al. studied a cyclic pursuit algorithm for multiple agents with motion constraints moving in a plane. Then in [3], Kim et al presented an on-line path generator design method based on a cyclic pursuit scheme to achieve target-enclosing. The 3-dimensional circular formation control was studied in [4] via set stabilization and a reduction principle for asymptotic stability of closed sets. Ref. [5] proposed a distributed control method combining attraction/repulsion from the neighbor agents and the target to circle on different obits for a group of unicycles. Ref. [6] discussed 3-types of the encirclement control for 3-dimensional space and also elaborated some issues about the collision-free motion and decentralized estimation. Ref. [7] proposed a distributed cyclic pursuit approach for target capture tasks using distance and bearing information through local sensing. The authors in [8] investigated the cyclic pursuit strategy to monitor a slowly moving target and validated the proposed control law by using aerial vehicles with bearing-only measurements. In [9] [10], the bearing-only circular formation were discussed.

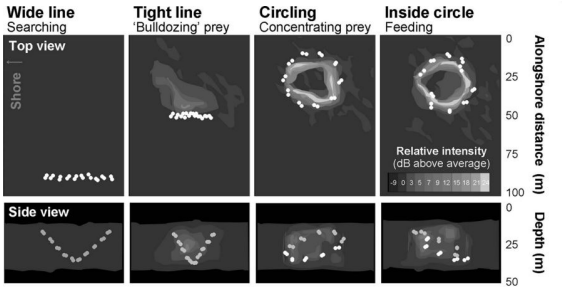

Fig. 1. Four stages of spinner dolphins to entrap the fishes

Recent years, the sophisticatedly cooperative hunting skill of spinner dolphins had been discovered through sonar techniques in [11]. As shown in Fig.1, on the "circling" stage, the spinner dolphins form a dynamic circle to entrap the targets as well as gradually tightening the encirclement to improve the concentration of the fishes. While the fishes are dense enough, pairs of dolphins at the opposite sides move inside the circle to feed themselves. The brilliant cooperation hunting behavior enlightens us to develop an encirclement approach to make the agents form a capturing formation pattern around targets, which can be widely applied in many areas such as coverage, patrolling and escorting etc. In this paper, we investigate the encirclement control problem with recently developed bearing rigidity [12]. The main contribution of this paper contains three aspects: firstly, we realize the bionic encirclement behavior as well as the tightening mechanism; secondly, to achieve the control objective, we design a distributed control law combining with bearing rigidity and consensus protocol; thirdly, we further figure out that the shrinkage of the formation scale is according to exponential law and also provide the estimates of the tightening rate.

The rest of the paper is organized as follows. Preliminaries are introduced in Section II. Section III gives the formulation of bearing-based bionic encirclement control problem. Then, in section IV, a control law based on bearing rigidity and consensus protocol is given. Further, we study the stability by using Lyapunov function and small gain theory. Simulation results are presented in Section V while the last section draws

This work is supported by National Key R&D Program of China (No.2017YFC0806500) and National Science Foundation of China (No.v1813205).

the conclusions.

II. Basic Notions and Preliminary Results

In this section, we briefly review some basic notions about graph theory and bearing rigidity.

Let $\mathcal{G} = (\mathcal{V}, \mathcal{E})$ be an undirected graph of order n specified by a node set $\mathcal{V} = \{v_1, \ldots, v_n\}$ and an edge set $\mathcal{E} \subseteq \mathcal{V} \times \mathcal{V}$ with size $m = |\mathcal{E}|$. The Cartesian coordination of vertex v_i in graph $\mathcal{G}$ is denoted as $p_i \in \mathbb{R}^d, (d \geq 2)$. Then vector $p = [(p_1)^T, \ldots, (p_n)^T]^T \in \mathbb{R}^{nd}$ is called a configuration of undirected graph $\mathcal{G}$ in $\mathbb{R}^d$. A framework in $\mathbb{R}^d$, denoted as $\mathcal{G}(p)$, is a combination of an undirected graph $\mathcal{G} = (\mathcal{V}, \mathcal{E})$ and a configuration p. In the framework $\mathcal{G}(p)$, we define:

$$\phi_{ij} \triangleq p_j - p_i, \quad g_{ij} = \phi_{ij}/\|\phi_{ij}\|, \forall (i,j) \in \mathcal{E} \tag{1}$$

where unit vector g_{ij} represents the relative bearing of p_j to p_i. Note $\phi_{ij} = -\phi_{ji}$ and thus $g_{ij} = -g_{ji}$. For a nonzero vector $\vec{v} \in \mathbb{R}^d (d \geq 2)$, define the operator $P : \mathbb{R}^d \to \mathbb{R}^{d \times d}$ as follows:

$$P(x) \triangleq I_d - \frac{\vec{v}}{\|\vec{v}\|} \frac{\vec{v}^T}{\|\vec{v}\|} \tag{2}$$

where matrix $I_d \in \mathbb{R}^{d \times d}$ represents the identity matrix and $\|\cdot\|$ represents Euclidian norm of a vector or the spectral norm of a matrix. Note $P(\vec{v})$ (denoted as $P_{\vec{v}}$ in the following content for notational simplicity) is an orthogonal projection operator. Any nonzero vector $\vec{v}$ will be projected onto its orthogonal compliment after the operation P. It can be easily verified that $P_{\vec{v}}$ satisfies $P_{\vec{v}}^2 = P_{\vec{v}}$ and $P_{\vec{v}}^H = P_{\vec{v}}$. This orthogonal projection operator is often used for verifying whether two vectors are parallel. For any two nonzero vectors $\vec{v}, \vec{u} \in \mathbb{R}^d$, if and only if $P_{\vec{v}}\vec{u} = 0$ (or equivalently $P_{\vec{u}}\vec{v} = 0$), they are parallel.

Consider an arbitrary orientation of the graph $\mathcal{G}(p)$ and denote the edge vector and the bearing for the kth directed edge as follows:

$$\phi_k \triangleq p_j - p_i, \quad g_k = \phi_{ij}/\|\phi_{ij}\|, \forall k \in 1, \ldots, m \tag{3}$$

Denote $\phi = [\phi_1^T, \ldots, \phi_m^T]^T$ and $g = [g_1^T, \ldots, g_m^T]^T$ in a compact form. Let $E \in \mathbb{R}^{m \times n}$ denotes the incidence matrix, where $[E]_{ki} = 1$ if vertex i is the head of edge k; $[E]_{ki} = -1$ if vertex i is the tail of edge k; $[E]_{ki} = 0$, otherwise.

The bearing function $F_B : \mathbb{R}^{dn} \to \mathbb{R}^{dm}$ is defined as

$$F_B(p) \triangleq [g_1^T, \ldots, g_m^T] \in \mathbb{R}^{dm} \tag{4}$$

The *bearing rigidity matrix* is defined as the Jacobian of the bearing function:

$$R_b(p) \triangleq \frac{\partial F_B(p)}{\partial p} \in \mathbb{R}^{dm \times dn}$$

Lemma 1 ([12]): A framework $\mathcal{G}(p)$ in $\mathbb{R}^d$ always satisfies $span\{1 \otimes I_d, p\} \subseteq Null(R_b(p))$ and $rank(R_b(p)) \leq dn - d - 1$.

Definition 1 (Infinitesimal Bearing Rigidity [12]): A framework is infinitesimally bearing rigid if all the infinitesimal bearing motions are trivial.

Lemma 2 (Condition for Infinitesimal Bearing Rigidity [12]): For a framework $\mathcal{G}$ in $\mathbb{R}^d$, the following statements are equivalent:
(a) $\mathcal{G}$ is infinitesimally bearing rigid;
(b) $rank(R(p)) = dn - d - 1$;
(c) $Null(R(p)) = span\{\mathbf{1}_n \otimes I_d, p\} = span\{1 \otimes I_d, p - \mathbf{1}_n \otimes \overline{p}\}$, where $\overline{p} = (1 \otimes I_d)^T p/n$ is the centroid of $\{p_i\}_{i \in \mathcal{V}}$.

The *Bearing Laplacian* $\mathcal{L}_b(\mathcal{G})$ can be represented as:

$$\mathcal{L}_b(\mathcal{G}) = (E^T \otimes I_d) diag(P_{ij}^*)(E \otimes I_d) \tag{5}$$

where E is the incidence matrix.

Lemma 3 ([13]): For an undirected graph $\mathcal{G}$, its Bearing Laplacian matrix $\mathcal{L}_b(\mathcal{G})$ has properties as follows:

1) $\mathcal{L}_b(\mathcal{G})$ is positive semi-definite and symmetrical;
2) $rank(\mathcal{L}_b(\mathcal{G}))) \leq dn - d - 1$ and $null(\mathcal{L}_b(\mathcal{G})) \supseteq span\{\mathbf{1}_n \otimes I_d, p\}$;
3) $rank(\mathcal{L}_b(\mathcal{G}))) = dn - d - 1$ and $null(\mathcal{L}_b(\mathcal{G})) = span\{\mathbf{1}_n \otimes I_d, p\}$ if and only if $\mathcal{G}(p)$ is infinitesimal bearing rigidity;

III. Problem Formulation of Bearing-based bionic Encirclement Control

A. Problem Formulation

Inspired by the cooperative prey of dolphins (as shown in Fig.2(a)), an analogous encirclement model is built using bearing theory. Supposed the dynamics of the i-th agent is represented by

$$\dot{p}_i = \mu_i, \quad i = 1, \ldots, n \tag{6}$$

where $p_i \in \mathbb{R}^d$ represents the position of agent i, and $\mu_i \in \mathbb{R}^d$ represents the control input. Let $p = [p_1^T, \ldots, p_n^T]^T \in \mathbb{R}^{nd}$ and $\mu = [\mu_1^T, \ldots, \mu_n^T]^T \in \mathbb{R}^{nd}$ represent the stack vector of positions and control inputs respectively. Considering a moving target T, its position and velocity are represented as p_t and $\dot{p}_t$. If target T can be detected by agent i, the relative bearing of agent i to target T can be represented as $g_{it} = (p_t - p_i)/\|p_t - p_i\|$.

Define the center and scale of multi-agent system as:

$$c(t) \triangleq \frac{1}{n}\sum_{i=1}^{n} p_i = \frac{1}{n}(1 \otimes I_d)^T p \tag{7}$$

$$s(t) \triangleq \sqrt{\frac{1}{n}\sum_{i=1}^{n} ||p_i - c(t)||^2} = \frac{1}{\sqrt{n}}||p - 1 \otimes c(t)|| \tag{8}$$

where operator $\otimes$ represents the Kronecker product. $c(t)$ and $s(t)$ represent the center and scale of the multi-agent system respectively.

The augmented graph $\hat{\mathcal{G}}$ consisting of n agents and target T is illustrated as Fig.2(b). The corresponding node set of augmented graph $\hat{\mathcal{G}}$ is $\hat{\mathcal{V}} = \{v_1, \ldots, v_n, v_{n+1}\}$ and the edge set is $\hat{\mathcal{E}} = \{e_1, \ldots, e_m, e_{m+1}, \ldots, e_{m+n}\}$.

To simplify the analysis, we are going to investigate the following target formation problem instead of studying the encirclement control problem directly.

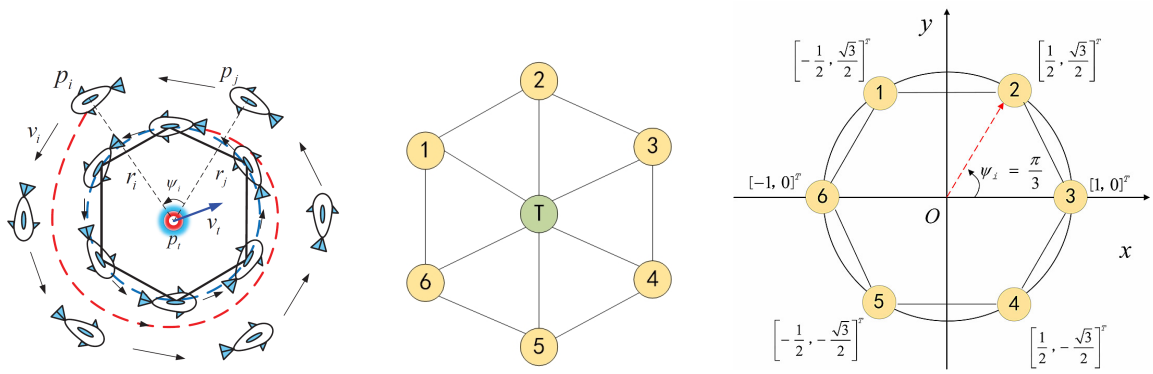

(a) The bionic mechanism of encirclement control. (b) The augmented graph $\hat{\mathcal{G}}$ with 6 agents and target T. (c) A regular polygon determined by bearing constraints

Fig. 2. The bionic mechanism of encirclement control

Definition 2 (Target Formation): If $\mathcal{G}(p(t))$ is graph of the target formation, it should satisfy following conditions:

1) bearing constraint: $g_{ij} // g^*_{ij}, g_{it} // g^*_{it}$;
2) formation center: $\lim_{t\to\infty} c(t) \to p_t(t)$;
3) formation scale: $\lim_{t\to\infty} s(t) \to 0$;

where the operator $//$ represents that two nonzero vectors are parallel. $g^*_{ij}(t)$ and $g^*_{it}(t)$ are time-varying bearing constraints. The geometric configuration determined by $g^*_{ij}(t)$ is a predefined regular polygon.

According to the definition of bearing rigidity in Definition 1, the augmented graph $\hat{\mathcal{G}}$ is infinitesimally bearing rigid. When the bearing constraint of each pair of neighbor nodes are given, the geometry configuration is determined (the shape is unique but the scale varies). Thus, we firstly assign n agents on unit circle evenly, and then calculate the inter-neighbor bearing constraints among agents $g^*_{ij}(0)$ and bearing constraints between agents and target $g^*_{it}(0)$ as defined in equation (1). A regular hexagon determined by bearing constraints is illustrated in Fig.2(c). We can check that the geometric configuration constrained by $\{g^*_{ij}(0)\}_{j\in\mathcal{N}_i} \bigcup \{g^*_{it}(0)\}_{i\in\mathcal{V}}$ is infinitesimal bearing rigidity. Thus, the framework can be uniquely determined up to a translational and a scaling factor, namely target's position and the formation's scale.

Further, rotation matrix $R(\theta)$ is introduced to achieve encirclement, where $\theta = \overline{w}t$ and $\overline{w}$ is the given angular velocity of formation. If $\overline{w} > 0$, the formation rotates anticlockwise. Otherwise, the formation rotates clockwise. Affected by rotation matrix, the formation's bearing constraint is time-varying. The bearing constraint at time t is given by $g^*_{ij}(t) = R(\theta)g^*_{ij}(0)$, $g^*_{it}(t) = R(\theta)g^*_{it}(0)$, where $g^*_{ij}(0)$ and $g^*_{it}(0)$ are initial bearing constraints at time 0.

IV. Bionic Encirclement Control Law Design and Stability Analysis

To solve the problem, the control law agent i is given as:

$$\mu_i = -k_\alpha \sum_{j\in N_i} P^*_{ij}(t)\left(p_i - p_j\right) - k_\beta P^*_{it}(t)\left(p_i - p_t\right) + \dot{p}_t, \tag{9}$$

in which, $k_\alpha > 0$, $k_\beta > 0$ are the gains; and $P^*_{ij}(t) = I_d - g^*_{ij}(t)\left(g^*_{ij}(t)\right)^T$, $P^*_{it}(t) = I_d - g^*_{it}(t)(g^*_{it}(t))^T$ are projection matrix defined by (2). Since the bearing constraints $g^*_{ij}(t)$ and $g^*_{it}(t)$ are time-variant, $P^*_{ij}(t)$ and $P^*_{it}(t)$ are also time-variant. Notice that $R(\theta)R(\theta)^T = I_d$, so we have $P^*_{ij}(t) = R(\theta)P^*_{ij}(0)R(\theta)^T$, $P^*_{it}(t) = R(\theta)P^*_{it}(0)R(\theta)^T$. According to the definition, the terms $P^*_{ij}(p_i - p_j)$ and $P^*_{it}(p_i - p_t)$ of the control law (9) are separately perpendicular to g^*_{ij} and g^*_{it}. Apparently, only the relative bearing information and relative position information are employed in (9), so that this control law is distributed. By using the control law (9), the whole system can be recast into the matrix form as follows:

$$\dot{p} = -k_\alpha \mathcal{L}_b(\mathcal{G})\, p - k_\beta \mathcal{D}_b(\mathcal{G})\left(p - \mathbf{1}_n \otimes p_t\right) + \mathbf{1}_n \otimes \dot{p}_t \tag{10}$$

in which, the matrix $\mathcal{L}_b(\mathcal{G}) \in \mathbb{R}^{dn\times dn}$ is bearing Laplacian. Besides, the matrix $\mathcal{D}_b(\mathcal{G}) = diag(P^*_{it}) \in \mathbb{R}^{dn\times dn}$ is a block diagonal matrix.

$$\begin{cases} [\mathcal{D}_b(\mathcal{G})]_{ij} = 0 & i \neq j; \\ [\mathcal{D}_b(\mathcal{G})]_{ij} = P^*_{it} & i = j; \end{cases} \tag{11}$$

$\mathcal{D}_b(\mathcal{G})$ is called as *target-bearing diagonal matrix*.

According to the property of projection matrix, we have $P^*_{ij} = P^{*2}_{ij}$ and $P^*_{ij} = P^{*T}_{ij}$, so that

$$\begin{aligned} \mathcal{L}_b(\mathcal{G}) &= (E \otimes I_d) diag\left(P^*_{ij}\right) diag\left(P^*_{ij}\right)(E^T \otimes I_d) \\ &= \tilde{R}_b(p^*)^T \tilde{R}_b(p^*). \end{aligned} \tag{12}$$

From the definition of bearing matrix $R_B(p^*) = diag\left(P^*_{g_{ij}}/\left\|e^*_{ij}\right\|\right)\left(E^T \otimes I_n\right)$, we know that $R_B(p^*)$ and $\tilde{R}_b(p^*)$ have the same rank and kernel space.

The stability proof of the encirclement control law (9) contains three steps.

Step 1: To prove $g_{ij} // g^*_{ij}$ and $g_{it} // g^*_{it}$

If g_{ij} and g^*_{ij} are parallel, we have $P^*_{ij} g_{ij} = 0$, where P^*_{ij} is an orthogonal projection matrix. And, if $g_{it} // g^*_{it}$, we have $P^*_{it} g_{it} = 0$.

Define $\eta = \tilde{R}_b(p^*)p$, in which $\tilde{R}_b(p^*)$ is the bearing rigidity matrix, denoted as $\tilde{R}_b^*$. Notice that $e = \left(E^T \otimes I_d\right) p$, then we have

$$\begin{aligned}\eta &= diag\left(P_{ij}^*\right)\left(E^T \otimes I_n\right) p \\ &= diag\left(\|e_k\| P_k^*\right)\left[\frac{e_1}{\|e_1\|}, \cdots, \frac{e_m}{\|e_m\|}\right]^T \\ &= diag\left(\|e_k\|\right)\left[P_1^* g_1, \cdots, P_m^* g_m\right]^T.\end{aligned}$$

Clearly, while $\eta \to 0$, $g_{ij}//g_{ij}^*$ is satisfied.

In a similar way, define $\xi = \mathcal{D}_b\left(p - \mathbf{1}_n \otimes p_t\right)$, where $\mathcal{D}_b$ is the target-bearing diagonal matrix. When $p_i \neq p_t$, $\xi \to 0$ implies $g_{it}//g_{it}^*$. Then, η and ξ can be used to analyze if the bearing constraints $g_{ij}//g_{ij}^*$ and $g_{it}//g_{it}^*$ are satisfied. Taking the derivative of η and applying (12), the η-subsystem is obtained

$$\dot{\eta} = -k_\alpha \tilde{R}_b^* \mathcal{L}_b p - k_\beta \tilde{R}_b^* \xi + \tilde{R}_b^*(\mathbf{1}_n \otimes \dot{p}_t).$$

According to Lemma 1, for any framework $\mathcal{G}(p)$, we have $null\left(\tilde{R}_b^*\right) \supset span\{\mathbf{1}_n \otimes I_d, p^*\}$, So that $\tilde{R}_b^*(\mathbf{1}_n \otimes \dot{p}_t) = 0$. Then, η-subsystem is

$$\dot{\eta} = -k_\alpha \tilde{R}_b^* \mathcal{L}_b p - k_\beta \tilde{R}_b^* \xi. \tag{13}$$

In the same way, ξ-subsystem can be obtained

$$\begin{aligned}\dot{\xi} &= -\mathcal{D}_b\Big(k_\alpha \mathcal{L}_b p + k_\beta \mathcal{D}_b\left(p - \mathbf{1}_n \otimes p_t\right)\Big) \\ &= -k_\beta \xi - k_\alpha \mathcal{D}_b(\tilde{R}_b^*)^T \eta.\end{aligned} \tag{14}$$

From (13) and (14), we can see that η-subsystem and ξ-subsystem form a typical interconnected feedback system.

For η-subsystem and ξ-subsystem, we respectively choose the following Lyapunov function $V_\eta = \frac{1}{2}\eta^T\eta$, $V_\xi = \frac{1}{2}\xi^T\xi$.

To prove η-subsystem and ξ-subsystem are input-to-state stable (ISS), the following lemma is given.

Lemma 4 ([14]): For a positive semi-definite matrix A, the minimum non-zero eigenvalue is denoted by $\lambda_2(A)$. The orthogonal complement space of $null\,(A)$ is represented by $null(A)^\perp$. For any vector $x \in null(A)^\perp$, we have $x^T A x \geq \lambda_2\,(A)\, x^T x$.

Next, we provide the following lemmas to prove that the η-subsystem and ξ-subsystem are ISS respectively.

Lemma 5: Applying the control law (9) for multi-agent network defined in Section III, then the η-subsystem taking ξ as input is ISS. In addition, for any $s \in \mathbb{R}_+$, the Lyapunov function V_η satisfies

$$V_\eta \geq \gamma_\xi^\eta\,(V_\xi) \Rightarrow \nabla V_\eta \dot{\eta} \leq -2\varepsilon V_\eta, \tag{15}$$

in which, for any constant $0 < \varepsilon < k_\alpha \lambda_2\,(\mathcal{L}_b)$, the interconnection gain $\gamma_\xi^\eta(s) = \left(\frac{k_\beta \left\|\tilde{R}_b^*\right\|}{k_\alpha \lambda_2(\mathcal{L}_b) - \varepsilon}\right)^2 s$.

Proof: By calculating the derivative of V_η along trajectory (13), we have

$$\dot{V}_\eta = -k_\alpha \eta^T \tilde{R}_b^*(\tilde{R}_b^*)^T \eta - k_\beta \eta^T \tilde{R}_b^* \xi. \tag{16}$$

Notice that $\tilde{R}_b^*(\tilde{R}_b^*)^T = \mathcal{L}_b^T$ is semi-definite. According to the definition of $\eta = \tilde{R}_b p$, we know that η belongs to the column space of $\tilde{R}_b$, i.e. equivalent to the orthogonal complement space $\eta \subset null\Big(\tilde{R}_b\Big)^\perp$ of the kernel space of $\tilde{R}_b$. According to Lemma 4, we have

$$\begin{aligned}\dot{V}_\eta &\leq -k_\alpha \lambda_2\,(\mathcal{L}_b)\,\|\eta\|^2 + k_\beta \|\eta\| \left\|\tilde{R}_b \xi\right\| \\ &\leq -\|\eta\| \left(k_\alpha \lambda_2\,(\mathcal{L}_b)\,\|\eta\| - k_\beta \left\|\tilde{R}_b\right\| \|\xi\|\right).\end{aligned} \tag{17}$$

For any given constant $0 < \varepsilon < k_\alpha \lambda_2\,(\mathcal{L}_b)$, from the gain condition that $V_\eta \geq \gamma_\xi^\eta\,(V_\xi)$, we obtain

$$\|\xi\| \leq \frac{k_\alpha \lambda_2\,(\mathcal{L}_b) - \varepsilon}{k_\beta \left\|\tilde{R}_b^*\right\|} \|\eta\|. \tag{18}$$

Bring (18) into (17), we have $\nabla V_\eta \dot{\eta} \leq -2\varepsilon V_\eta$. ■

Lemma 6: Applying the control law (9) for multi-agent network defined in Section III, then ξ-subsystem taking η as input is ISS. In addition, for any $s \in \mathbb{R}_+$, the Lyapunov function V_η satisfies

$$V_\xi \geq \gamma_\eta^\xi\,(V_\eta) \Rightarrow \nabla V_\xi \dot{\xi} \leq -2\tau V_\xi, \tag{19}$$

in which, for any constant $0 < \tau < k_\beta$, the interconnection gain $\gamma_\eta^\xi\,(s) = \left(\frac{k_\alpha}{k_\beta - \tau}\left\|\mathcal{D}_b \tilde{R}_b^*\right\|\right)^2 s$.

Proof: Similar to the proof of Lemma 8. ■

Finally, we prove the bearing constraint can be satisfied by using control law (9) under the following lemma.

Lemma 7: By applying control law (9), if the small gain condition

$$\gamma_\xi^\eta \circ \gamma_\eta^\xi < Id, \tag{20}$$

is satisfied, the composite system constructed by η-subsystem and ξ-subsystem is globally asymptotically stable, i.e. $\eta \to 0$, $\xi \to 0$. Finally, the bearing constraint $g_{ij}//g_{ij}^*$, $g_{it}//g_{it}^*$ can be satisfied.

Proof: According to the classic small gain theorem, when the gain of the interconnection subsystem satisfies

$$\gamma_\xi^\eta \circ \gamma_\eta^\xi < Id,$$

the composite system constructed by η-subsystem and ξ-subsystem is ISS. As we known, zero-input ISS system is globally asymptotically stable, so that the composite system constructed by η-subsystem and ξ-subsystem is also globally asymptotically stable as well as $g_{ij}//g_{ij}^*$, $g_{it}//g_{it}^*$. ■

Step 2: to prove $\lim_{t\to\infty} c\,(t) \to p_t$;

In order to prove that the multi-agent formation has the ability to track the target $\lim_{t\to\infty} c\,(t) \to p_t$, we give the following lemma.

Lemma 8: For the augmented multi-agent network $\hat{\mathcal{G}}$ described in Section III, taking the control law (9) as input, the formation can track the moving target and $\lim_{t\to\infty} c^*\,(t) \to p_t$.

Proof: The error between the center of formation and the target position is $\delta = c - p_t$. By calculating the derivation of δ, we obtain

$$\begin{aligned}\dot{\delta} &= -\frac{1}{n}(\mathbf{1}_n \otimes I_d)^T \left(k_\beta \mathcal{D}_b\left(p - \mathbf{1}_n \otimes p_t\right)\right) \\ &= -\frac{k_\beta}{n}(\mathbf{1}_n \otimes I_d)^T \xi.\end{aligned} \tag{21}$$

Then, it can be seen that the composite system is kind of serial interconnection of δ-subsystem and ξ-subsystem.

From equation (21), we know that δ-subsystem is a linear system with only input term, so that it is ISS. According to Lemma 6, ξ-subsystem is ISS and globally asymptotically stable, which means that the composite system constructed by δ-subsystem and ξ-subsystem is also globally asymptotically stable, in that way $\lim_{t\to\infty} c(t) \to p_t$. ■

Step 3: to prove $\lim_{t\to\infty} s(t) \to 0$**.**

Define the formation scale $\hat{s}(t)$ about target T as follows:

$$\hat{s}(t) = \frac{1}{\sqrt{n}} \|p - \mathbf{1}_n \otimes p_t\|. \tag{22}$$

In this section, we are going to investigate the change rate of $\hat{s}(t)$ instead of $s(t)$.

Lemma 9: For the augmented multi-agent network $\hat{\mathcal{G}}$ described in Section III, taking the control law (9) as input, then the formation scale $\hat{s}(t)$ will not further increase.

Proof: Because $\mathcal{L}_b$ and $\mathcal{D}_b$ are semi-definite, by taking the derivative of $\hat{s}(t)$ along trajectory (10), obtain

$$\begin{aligned}\dot{\hat{s}}(t) &= \frac{1}{\sqrt{n}} \frac{(p - \mathbf{1}_n \otimes p_t)^T}{\|p - \mathbf{1}_n \otimes p_t\|} (\dot{p} - \mathbf{1}_n \otimes \dot{p}_t) \\ &= -\frac{1}{\sqrt{n}} \frac{(p - \mathbf{1}_n \otimes p_t)^T}{\|p - \mathbf{1}_n \otimes p_t\|} (k_\alpha \mathcal{L}_b + k_\beta \mathcal{D}_b)(p - \mathbf{1}_n \otimes p_t) \\ &\le 0. \end{aligned} \tag{23}$$

So, the formation scale $\hat{s}(t)$ will not further increase. In addition, we have $\hat{s}(t) \le \hat{s}(0),\ t \ge 0$. ■

For convenience, define the orthogonal projection matrix as follows:

$$\begin{aligned} Q_M &= (\mathbf{1}_n \otimes I_d)\left((\mathbf{1}_n \otimes I_d)^T (\mathbf{1}_n \otimes I_d)\right)(\mathbf{1}_n \otimes I_d)^T \\ &= \begin{bmatrix} \frac{1}{n} & \cdots & \frac{1}{n} \\ \vdots & \ddots & \vdots \\ \frac{1}{n} & \cdots & \frac{1}{n} \end{bmatrix} \otimes I_d. \end{aligned} \tag{24}$$

The function of the matrix is to project an arbitrary vector into the subspace of $span\{\mathbf{1}_n \otimes I_d\}$. Correspondingly, the orthogonal projection matrix of $span\{\mathbf{1}_n \otimes I_d\}^\perp$ is defined as

$$Q_M{}^\perp = I_n \otimes I_d - Q_M = \begin{bmatrix} 1 - \frac{1}{n} & \cdots & -\frac{1}{n} \\ \vdots & \ddots & \vdots \\ -\frac{1}{n} & \cdots & 1 - \frac{1}{n} \end{bmatrix} \otimes I_d. \tag{25}$$

For the orthogonal projection matrix, we have

$$Q_M = Q_M^2, Q_M{}^\perp = (Q_M{}^\perp)^2, Q_M Q_M{}^\perp = Q_M{}^\perp Q_M = \mathbf{0}_n. \tag{26}$$

According to the definition of the center $c(t) = \frac{1}{n}(\mathbf{1}_n \otimes I_d)^T p$, we have

$$p - \mathbf{1}_n \otimes c(t) = p - Q_M p = Q_M{}^\perp p, \tag{27}$$

Finally, the formation scale can be addressed as

$$s(t) = \frac{1}{\sqrt{n}} \left\|Q_M^\perp p\right\|. \tag{28}$$

Choose the following Lyapunov function

$$V_s = s(t). \tag{29}$$

Next, we will discuss the change rate of the formation scale $s(t)$ through the following lemma.

Lemma 10: Considering the augmented multi-agent network $\hat{\mathcal{G}}$ described in Section III, when taking the control law (9) as input, the formation scale $s(t)$ will converge according to exponential law, i.e. $\lim_{t\to\infty} s(t) \to 0$. The rate of shrinking can be estimated as follows:

$$s(t) \le e^{-\frac{k_\alpha}{\sqrt{n}}\lambda_2(\mathcal{L}_b)t} s(0), \quad t \ge 0. \tag{30}$$

Proof: From lemma 3, we know that the subspace of $span\{\mathbf{1}_n \otimes I_d, p\}$ belongs to the kernel of bearing Laplacian $\mathcal{L}_b$, so that $\mathcal{L}_b(\mathbf{1_n} \otimes c(t)) = 0$. Next, by taking the derivative of $s(t)$, we obtain

$$\begin{aligned} \dot{s}(t) &= \frac{1}{\sqrt{n}} \frac{\left(Q_M^\perp p\right)^T}{\left\|Q_M^\perp p\right\|} (I_n - Q_M)\dot{p} = \frac{1}{\sqrt{n}} \frac{\left(Q_M^\perp p\right)^T}{\left\|Q_M^\perp p\right\|} \dot{p} \\ &= -\frac{k_\alpha}{\sqrt{n}} \frac{\left(Q_M^\perp p\right)^T}{\left\|Q_M^\perp p\right\|} \mathcal{L}_b \left(Q_M^\perp p\right) - \frac{k_\beta}{\sqrt{n}} \frac{\left(Q_M^\perp p\right)^T}{\left\|Q_M^\perp p\right\|} \mathcal{D}_b Q_M^\perp p \\ &\quad - \frac{k_\beta}{\sqrt{n}} \frac{\left(Q_M^\perp p\right)^T}{\left\|Q_M^\perp p\right\|} \mathbf{1}_n \otimes \delta. \end{aligned}$$

From the property of the orthogonal projection matrix, it is known that $Q_M^\perp p$ belongs to the orthogonal complement subspace of the kernel space of $\mathcal{L}_b$. From 4, we have

$$\left(Q_M^\perp p\right)^T \mathcal{L}_b \left(Q_M^\perp p\right) \ge \lambda_2(\mathcal{L}_b) \left\|Q_M^\perp p\right\|$$

The target-bearing diagonal matrix $\mathcal{D}_b$ is a symmetric semi-definite matrix, so that

$$\left(Q_M^\perp p\right)^T D_b \left(Q_M^\perp p\right) \ge 0. \tag{31}$$

Taking the derivative of V_s along trajectory (31). Noticed that δ-subsystem is globally asymptotically stable, i.e. $\delta \to 0$, obtain

$$\begin{aligned} \dot{V}_s &\le -\frac{k_\alpha}{\sqrt{n}} \lambda_2(\mathcal{L}_b)\, s + \frac{k_\beta}{\sqrt{n}} \|\mathbf{1}_n \otimes \delta\| \\ &\le \underbrace{-\frac{k_\alpha}{\sqrt{n}} \lambda_2(\mathcal{L}_b)\, s}_{s_1} + \underbrace{k_\beta \|\delta\| \to 0}_{s_2}. \end{aligned} \tag{32}$$

Obviously, when s_2 converges towards 0, the convergence speed of $s(t)$ is dominated by s_1.

$$\dot{V}_s(s(t)) \le -\frac{k_\alpha}{\sqrt{n}} \lambda_2(\mathcal{L}_b)\, V_s(s(t)) \tag{33}$$

$s(t)$ will converge to the equilibrium point exponentially.

By using comparison lemma, we have

$$V_s(s(t)) \le e^{-\frac{k_\alpha}{\sqrt{n}}\lambda_2(\mathcal{L}_b)t} V_s(s(0)), \quad t \ge 0, \tag{34}$$

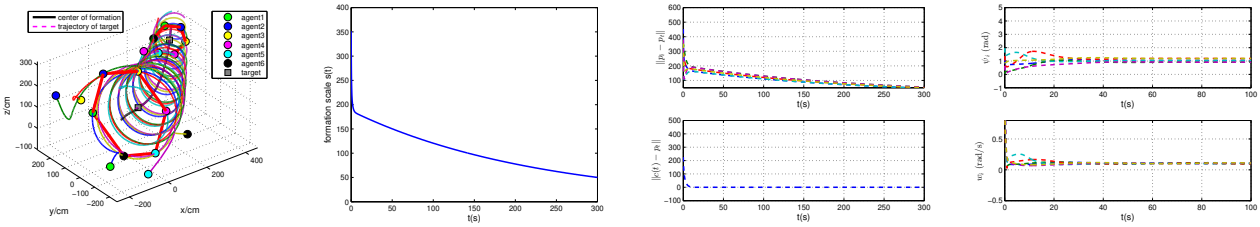

(a) The agents encircle a specific moving target in 3D space.

(b) The formation scale $s(t)$.

(c) The distance error of p_t and the formation center.

(d) The angle of neighbours Ψ_i and the rotation speed w_i.

Fig. 3. The simulation results under the distributed control law (9).

Besides, the estimation of the shrinking rate is

$$s\left(t\right) \leq e^{-\frac{k_\alpha}{\sqrt{n}}\lambda_2(\mathcal{L}_b)t} s\left(0\right), \quad t \geq 0.$$

■

Combining Lemma 8-10, we can come to the main conclusion of this chapter.

Theorem 1: Considering the augmented multi-agent network $\hat{\mathcal{G}}$ described in Section III, when taking the control law (9) as input, the following control objectives can be achieved: $g_{ij}//g_{ij}^*$, $g_{it}//g_{it}^*$; $\lim\limits_{t\to\infty} c\left(t\right) \to p_t$; $\lim\limits_{t\to\infty} s\left(t\right) \to 0$. So that the multi-agent system can encircle the moving target T.

V. Simulation

In this section, simulation experiments are performed to validate the effectiveness of the control law.

In 3D space, the rotation matrix about i_ρ can be defined as $R\left(\theta\right) = \left(\cos\left(\theta\right)\right) I_3 + \left(1 - \cos\left(\theta\right)\right) i_\rho i_\rho^T + \left(\sin\left(\theta\right)\right) \left[i_\rho\right]_\times$, where $\theta = \bar{w}t$ and $\bar{w} = -\frac{\pi}{30}\ (rad/s)$. Set $i_\rho = [0, 0, 1]^T$ and the position as well as the velocity of target as $p_t = [100,\ 100,\ 50]^T\ cm$, $\dot{p}_t = [1,\ 0.05 * (t/15),\ 0.05 * (t/10)]^T\ cm/s$, respectively. The initial position of agents are given as $[-250,\ -186,\ 30]^T\ cm$, $[-220,\ 220,\ 170]^T\ cm$, $[-140,\ 155,\ 150]^T\ cm$, $[150,\ 110,\ 300]^T\ cm$, $[-80,\ -220,\ -50]^T\ cm$, $[100,\ -250,\ 90]^T\ cm$. Choose $k_\alpha = 1.75$, $k_\beta = 1.0$. By implementing the control law (9), the results are shown in Fig.3(a)-3(d). In Fig.3(a), the agents achieve an encirclement behavior to surround the target. In addition, during tracking the target, the formation is gradually tightening. From Fig.3(c), we can see that the errors between formation center and the target is gradually converging to zero.

VI. Conclusions

In this paper, we investigated the bionic encirclement control of multi-agent system inspired by the effective cooperative prey of dolphins. By combining bearing rigidity theory and consensus protocol, we proposed a distributed control law to achieve the encirclement behavior. The agents are able to enclose a specific moving target and finally form a ring of encirclement to prevent the escape of the target. Specifically, we figured out that the shrinkage of the formation scale is according to exponential law and also provided the estimates of the rate.

References

[1] J. K. Parrish, S. V. Viscido, and D. Grünbaum, "Self-organized fish schools: an examination of emergent properties," *The biological bulletin*, vol. 202, no. 3, pp. 296–305, 2002.

[2] J. A. Marshall, M. E. Broucke, and B. A. Francis, "Formations of vehicles in cyclic pursuit," *IEEE Transactions on automatic control*, vol. 49, no. 11, pp. 1963–1974, 2004.

[3] T.-H. Kim, S. Hara, and Y. Hori, "Cooperative control of multi-agent dynamical systems in target-enclosing operations using cyclic pursuit strategy," *International Journal of Control*, vol. 83, no. 10, pp. 2040–2052, 2010.

[4] M. I. El-Hawwary, "Three-dimensional circular formations via set stabilization," *Automatica*, vol. 54, pp. 374–381, 2015.

[5] R. Zheng, Z. Lin, M. Fu, and D. Sun, "Distributed control for uniform circumnavigation of ring-coupled unicycles," *Automatica*, vol. 53, pp. 23–29, 2015.

[6] A. Franchi, P. Stegagno, and G. Oriolo, "Decentralized multi-robot encirclement of a 3d target with guaranteed collision avoidance," *Autonomous Robots*, pp. 1–21, 2015.

[7] T.-H. Kim and T. Sugie, "Cooperative control for target-capturing task based on a cyclic pursuit strategy," *Automatica*, vol. 43, no. 8, pp. 1426–1431, 2007.

[8] J. O. Swartling, I. Shames, K. H. Johansson, and D. V. Dimarogonas, "Collective circumnavigation," *Unmanned Systems*, vol. 2, no. 03, pp. 219–229, 2014.

[9] R. Zheng, Y. Liu, and D. Sun, "Enclosing a target by nonholonomic mobile robots with bearing-only measurements," *Automatica*, vol. 53, pp. 400–407, 2015.

[10] S. Daingade and A. Sinha, "Target centric cyclic pursuit using bearing angle measurements only," in *Advances in Control and Optimization of Dynamical Systems*, vol. 3, pp. 491–496, 2014.

[11] K. J. Benoit-Bird and W. W. Au, "Cooperative prey herding by the pelagic dolphin, stenella longirostris," *The Journal of the Acoustical Society of America*, vol. 125, no. 1, pp. 125–137, 2009.

[12] S. Zhao and D. Zelazo, "Bearing rigidity and almost global bearing-only formation stabilization," *IEEE Transactions on Automatic Control*, vol. 61, no. 5, pp. 1255–1268, 2016.

[13] S. Zhao and D. Zelazo, "Localizability and distributed protocols for bearing-based network localization in arbitrary dimensions," *Automatica*, vol. 69, pp. 334–341, 2016.

[14] X. Wang, T. Liu, and J. Qin, "Second-order consensus with unknown dynamics via cyclic-small-gain method," *IET Control Theory & Applications*, vol. 6, no. 18, pp. 2748–2756, 2012.